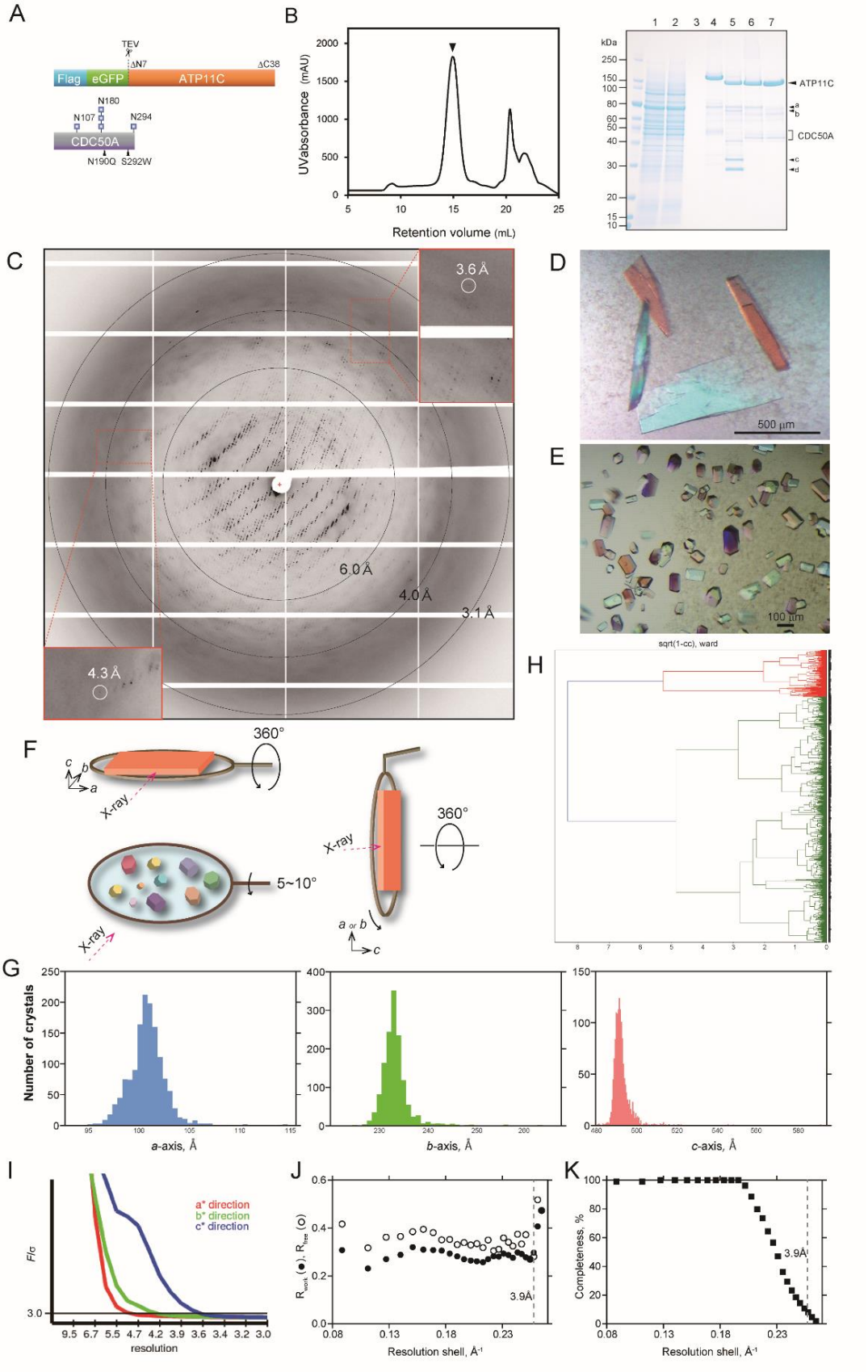
A
TEV
ΔN7
ΔC38
Flag
eGFP
ATP11C
N180
N107
N294
CDC50A
N190Q
S292W
B
UVabsorbance (mAU)
Retention volume (mL)
1 2 3 4 5 6 7
kDa
ATP11C
CDC50A
C
3.6 Å
6.0 Å
4.0 Å
3.1 Å
4.3 Å
D
500 μm
E
100 μm
H
sqrt(1-cc), ward
F
360°
X-ray
5~10°
a or b
c
G
Number of crystals
a-axis, Å
b-axis, Å
c-axis, Å
I
a* direction
b* direction
c* direction
I/σ
resolution
J
Rwork (●), Rfree (○)
3.9Å
Resolution shell, Å-1
K
Completeness, %
3.9Å
Resolution shell, Å-1

Fig. S1. Structural determination of ATP11C-CDC50A complex

(**A**) Construction of TP11C and CDC50A used in crystallization. See Methods for details. (**B**) Purification of ATP11C-CDC50A complex. Lane 1: solubilized cell lysate, lane 2: pass-through of Flag resin, lane 3: wash fraction, lane 4: elution by Flag peptide (subjected to ATPase assay), lane 5: TEV proteinase- and endoglycosidase-treated sample, lane 6: pass-through fraction of Ni-NTA and amylose resin, lane 7: concentrated peak fractions by size-exclusion chromatography (arrowhead in the left panel). Arrowheads on the right indicate as follows, a: HSP70, b: EndoHf, c: cleaved eGFP, d: TEV proteinase. The elution profile of ATP11C-CDC50A complex by size-exclusion column chromatography is shown on the left. (**C**) Representative X-ray diffraction obtained from a plate-like crystal shown in **D**. Diffraction spots better than 3.6Å were obtained along the c^*-axis, whereas these are limited to around 4~6Å in directions along the a^*- and b^*-axes, thus strongly anisotropic. (**D**,**E**) Three-dimensional crystals obtained from the samples purified from Expi293 cells, showing thin, but large plate-like crystals (**D**). In contrast, small crystals were obtained from CDC50A-KO cells (**E**). (**F**) Data acquisition strategy. We employed normal type LithoLoops for helical scan data acquisition from large single crystals. However, because crystals showed strong anisotropy, we also collected data sets by irradiating the X-ray beam from the direction perpendicular to the *c*-axis using 90º bent type LithoLoops. For the small but well diffracting crystals obtained from CDC50A-KO cells, data from each individual crystal were collected for 10º. All of these crystals showed identical unit cell size and symmetry regardless of crystal morphologies and expression cell types, as seen in the histograms of unit cell dimensions (**G**). (**H**) The result of correlation coefficient (CC) based clustering of data sets by *KAMO*. $[1 - \mathrm{CC}(i,j)]^{1/2}$ was used as a distance between two data sets i and j, where $\mathrm{CC}(i,j)$ denotes the CC of intensity (52). The vertical axis represents 1,588 data sets, whereas the horizontal axis represents the distances between clusters. All diffraction data were finally merged into a single data set, and used for the molecular replacement. (**I**) F/σ is plotted for the three principle directions of the crystal using Diffraction Anisotropy Server. $R_{\mathrm{work}}/R_{\mathrm{free}}$ (**J**) and completeness (K) are plotted for the analyzed resolution shells. Dotted grey lines indicate the highest resolution shell (3.9Å) for the present structural analysis.

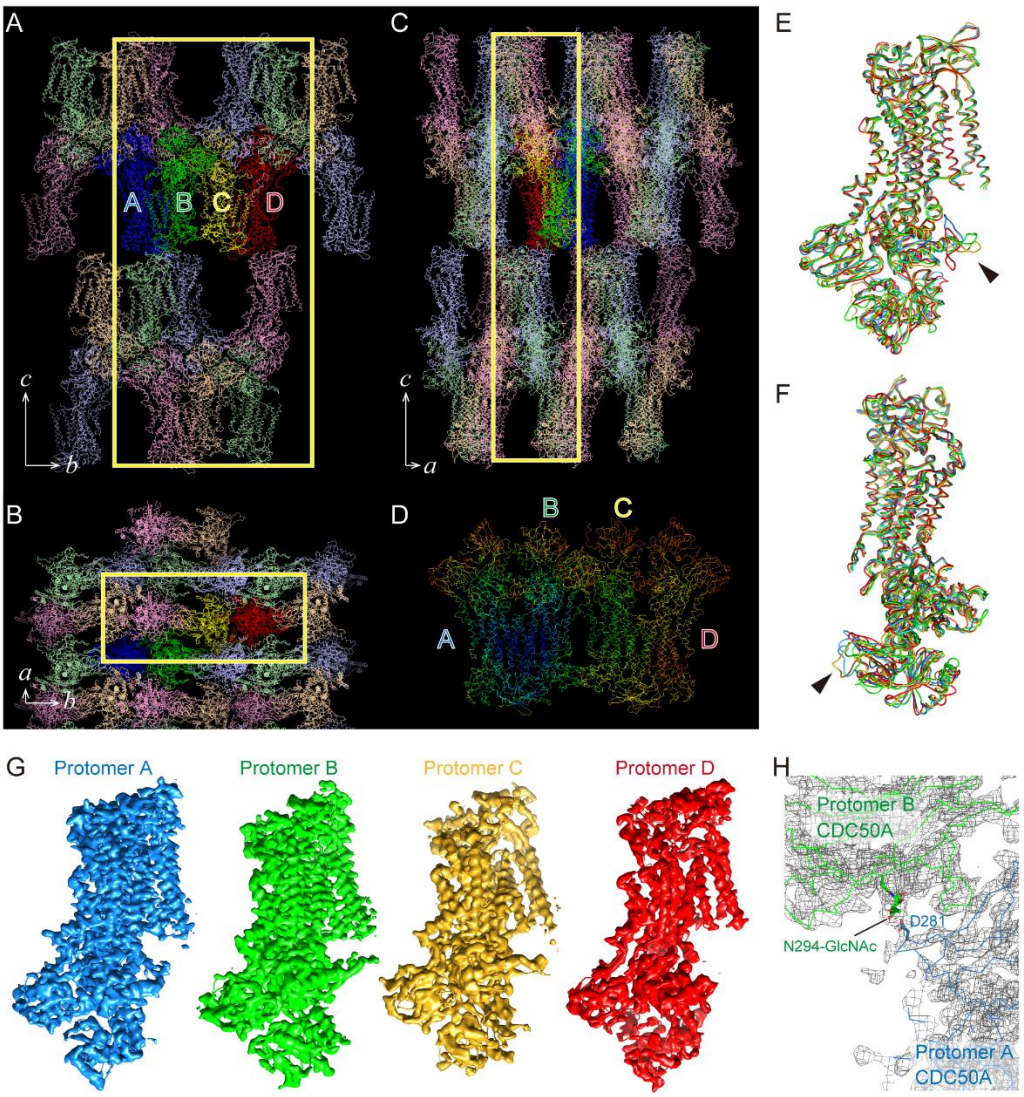

Fig. S2. Crystal packing.

(**A**-**C**) An asymmetric unit contains four protomers (A, B, C and D) shown in blue, green, yellow and red, respectively. Their symmetry-related molecules are shown in light colors. Yellow boxes indicate unit cells viewed from different directions in **A**-**C** as indicated in the figures. (**D**) Molecules in the asymmetric unit are displayed according to their temperature factors. Colors gradually change from blue (16) to red (283). (**E**,**F**) Comparison of the molecular conformation of four protomers. Arrowheads indicate loop structures, the conformations of which are variable among the four protomers. (**G**) $2F_o$-F_c electron density maps of the four protomers at the same contour level of 1.5σ. (H) Close-up view of a crystal contact site at the interface of CDC50A subunit of protomer A (blue) and protomer B (green) achieved by a GlcNAc attached to $Asn294^{CDC50A}$. Grey mesh represents $2F_o$-F_c map with 1.5σ contour level.

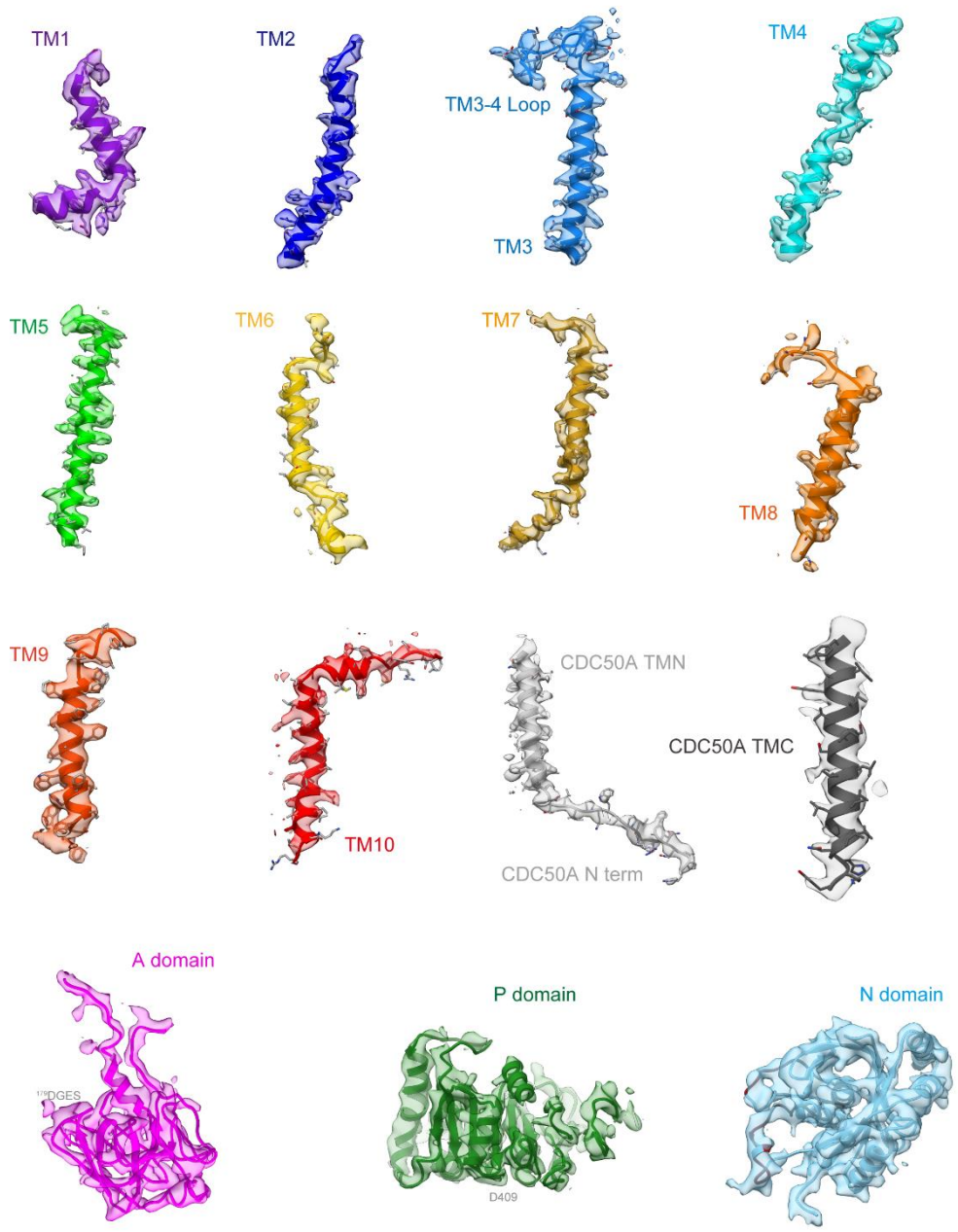

Fig. S3. Electron density maps
Surface represents $2F_o$-F_c electron density maps of the indicated regions with 1.5σ contour level. Color code as in Fig. 1.

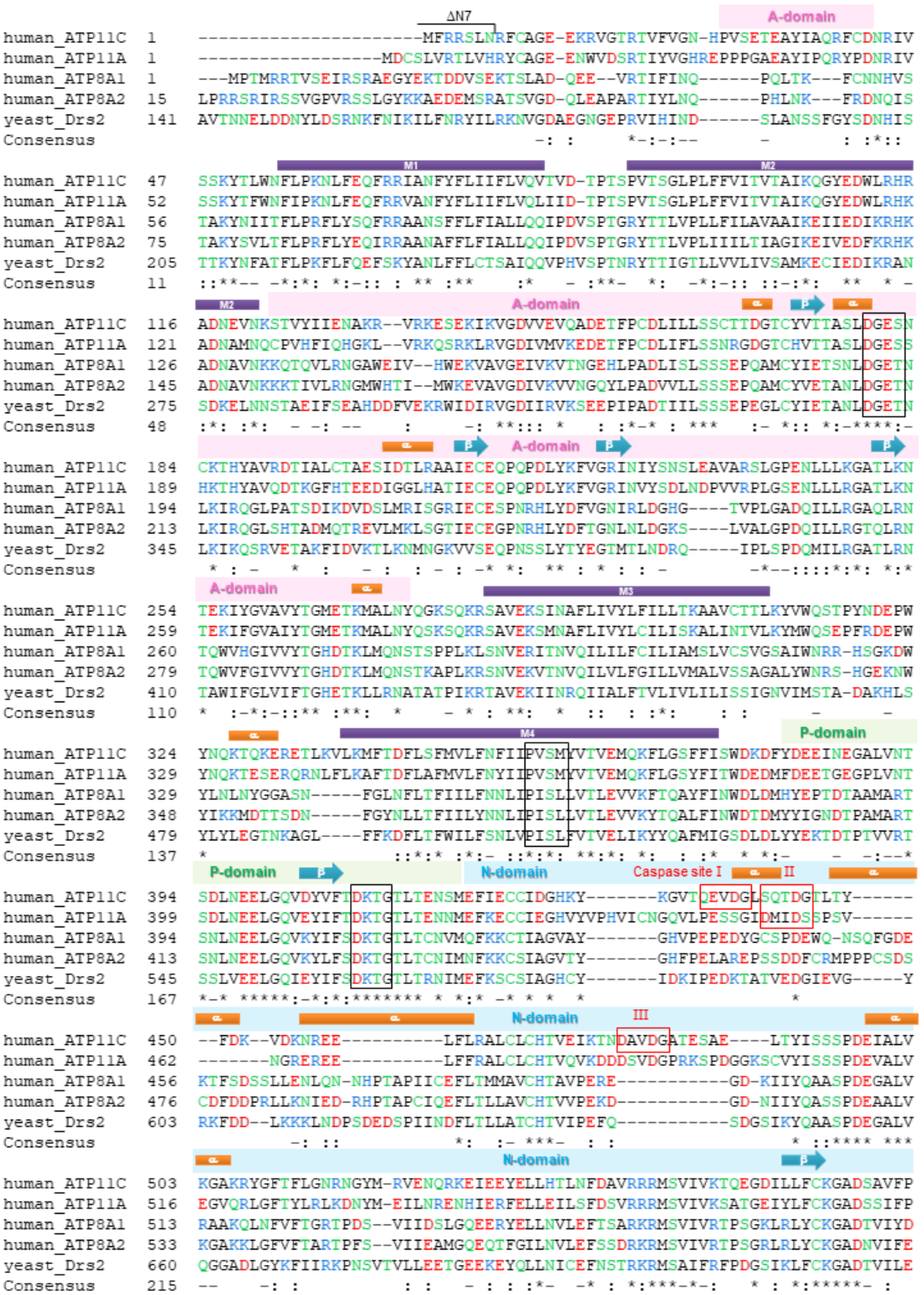
ΔN7
A-domain
M1
M2
M3
M4
P-domain
N-domain
Caspase site I
II
III
human_ATP11C
human_ATP11A
human_ATP8A1
human_ATP8A2
yeast_Drs2
Consensus

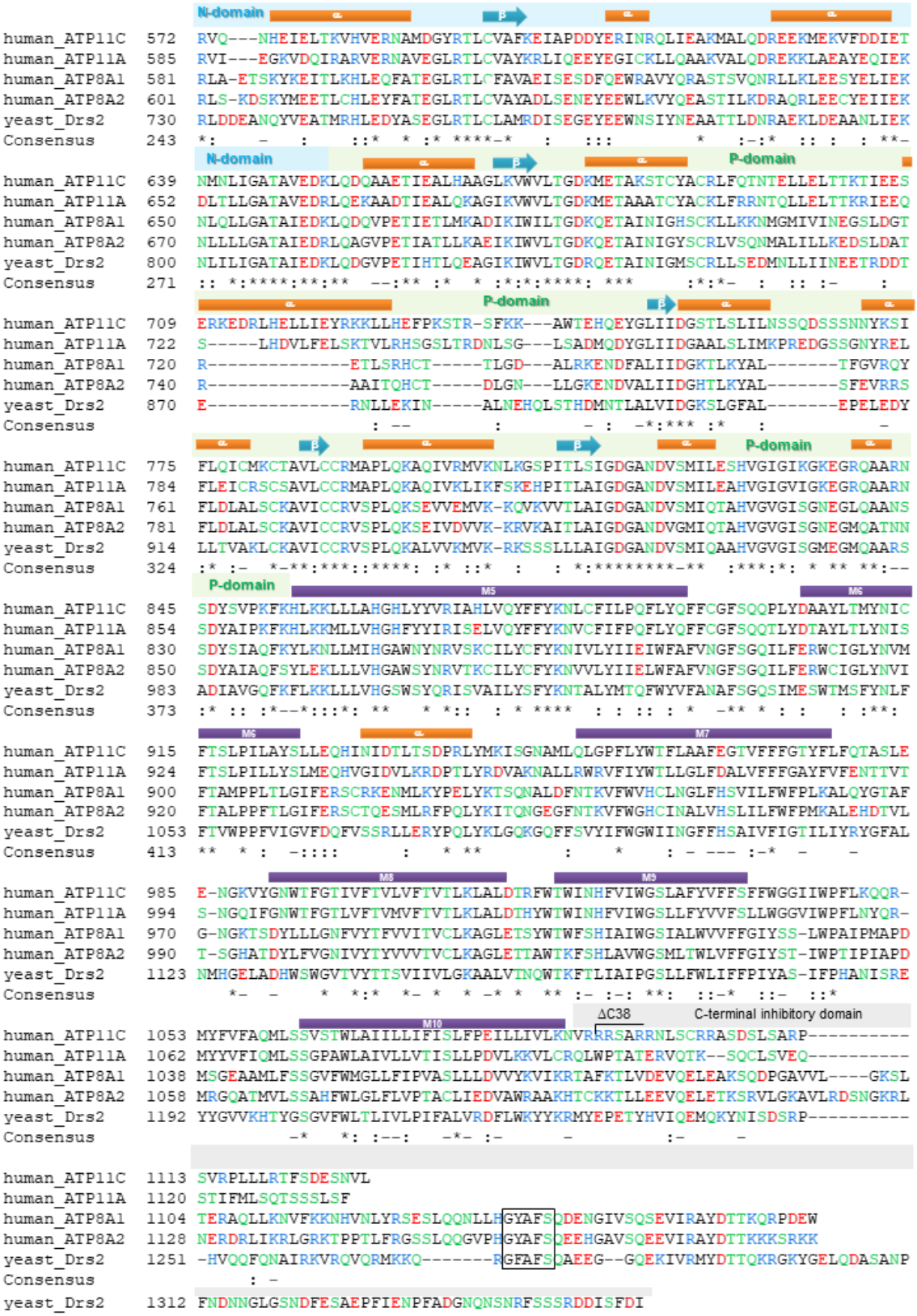
N-domain
P-domain
M5
M6
M7
M8
M9
M10
ΔC38
C-terminal inhibitory domain
human_ATP11C 572 RVQ---NHEIELTKVHVERNAMDGYRTLCVAFKEIAPDDYERINRQLIEAKMALQDREEKMEKVFDDIET
human_ATP11A 585 RVI---EGKVDQIRARVERNAVEGLRTLCVAYKRLIQEEYEGICKLLQAAKVALQDREKKLAEAYEQIEK
human_ATP8A1 581 RLA-ETSKYKEITLKHLEQFATEGLRTLCFAVAEISESDFQEWRAVYQRASTSVQNRLLKLEESYELIEK
human_ATP8A2 601 RLS-KDSKYMEETLCHLEYFATEGLRTLCVAYADLSENEYEEWLKVYQEASTILKDRAQRLEECYEIIEK
yeast_Drs2 730 RLDDEANQYVEATMRHLEDYASEGLRTLCLAMRDISEGEYEEWNSIYNEAATTLDNRAEKLDEAANLIEK
Consensus 243 *: - : ::* * :* ****-* : ::: * :-:* :: : : **-
human_ATP11C 639 NMNLIGATAVEDKLQDQAAETIEALHAAGLKVWVLTGDKMETAKSTCYACRLFQTNTELLELTTKTIEES
human_ATP11A 652 DLTLLGATAVEDRLQEKAADTIEALQKAGIKVWVLTGDKMETAAATCYACKLFRRNTQLLELTTKRIEEQ
human_ATP8A1 650 NLQLLGATAIEDKLQDQVPETIETLMKADIKIWILTGDKQETAINIGHSCKLLKKNMGMIVINEGSLDGT
human_ATP8A2 670 NLLLLGATAIEDRLQAGVPETIATLLKAEIKIWVLTGDKQETAINIGYSCRLVSQNMALILLKEDSLDAT
yeast_Drs2 800 NLILIGATAIEDKLQDGVPETIHTLQEAGIKIWVLTGDRQETAINIGMSCRLLSEDMNLLIINEETRDDT
Consensus 271 :: *:****:**:** --:** :* * :*:*:****: *** :*:*- : :: :- :
human_ATP11C 709 ERKEDRLHELLIEYRKKLLHEFPKSTR-SFKK---AWTEHQEYGLIIDGSTLSLILNSSQDSSSNNYKSI
human_ATP11A 722 S-----LHDVLFELSKTVLRHSGSLTRDNLSG---LSADMQDYGLIIDGAALSLIMKPREDGSSGNYREL
human_ATP8A1 720 R--------------ETLSRHCT-----TLGD---ALRKENDFALIIDGKTLKYAL-------TFGVRQY
human_ATP8A2 740 R--------------AAITQHCT-----DLGN---LLGKENDVALIIDGHTLKYAL-------SFEVRRS
yeast_Drs2 870 E--------------RNLLEKIN-----ALNEHQLSTHDMNTLALVIDGKSLGFAL-------EPELEDY
Consensus : -- : - : -*:*** :* : -
human_ATP11C 775 FLQICMKCTAVLCCRMAPLQKAQIVRMVKNLKGSPITLSIGDGANDVSMILESHVGIGIKGKEGRQAARN
human_ATP11A 784 FLEICRSCSAVLCCRMAPLQKAQIVKLIKFSKEHPITLAIGDGANDVSMILEAHVGIGVIGKEGRQAARN
human_ATP8A1 761 FLDLALSCKAVICCRVSPLQKSEVVEMVK-KQVKVVTLAIGDGANDVSMIQTAHVGVGISGNEGLQAANS
human_ATP8A2 781 FLDLALSCKAVICCRVSPLQKSEIVDVVK-KRVKAITLAIGDGANDVGMIQTAHVGVGISGNEGMQATNN
yeast_Drs2 914 LLTVAKLCKAVICCRVSPLQKALVVKMVK-RKSSSLLLAIGDGANDVSMIQAAHVGVGISGMEGMQAARS
Consensus 324 :* :- *-**:***::****: :* ::* : : *:********-** :***:*: * ** **:--
human_ATP11C 845 SDYSVPKFKHLKKLLLAHGHLYYVRIAHLVQYFFYKNLCFILPQFLYQFFCGFSQQPLYDAAYLTMYNIC
human_ATP11A 854 SDYAIPKFKHLKKMLLVHGHFYYIRISELVQYFFYKNVCFIFPQFLYQFFCGFSQQTLYDTAYLTLYNIS
human_ATP8A1 830 SDYSIAQFKYLKNLLMIHGAWNYNRVSKCILYCFYKNIVLYIIEIWFAFVNGFSGQILFERWCIGLYNVM
human_ATP8A2 850 SDYAIAQFSYLEKLLLVHGAWSYNRVTKCILYCFYKNVVLYIIELWFAFVNGFSGQILFERWCIGLYNVI
yeast_Drs2 983 ADIAVGQFKFLKKLLLVHGSWSYQRISVAILYSFYKNTALYMTQFWYVFANAFSGQSIMESWTMSFYNLF
Consensus 373 :* :: :*--*:::*: ** * *:: : * **** : : :: : * -** * : : : :**:
human_ATP11C 915 FTSLPILAYSLLEQHINIDTLTSDPRLYMKISGNAMLQLGPFLYWTFLAAFEGTVFFFGTYFLFQTASLE
human_ATP11A 924 FTSLPILLYSLMEQHVGIDVLKRDPTLYRDVAKNALLRWRVFIYWTLLGLFDALVFFFGAYFVFENTTVT
human_ATP8A1 900 FTAMPPLTLGIFERSCRKENMLKYPELYKTSQNALDFNTKVFWVHCLNGLFHSVILFWFPLKALQYGTAF
human_ATP8A2 920 FTALPPFTLGIFERSCTQESMLRFPQLYKITQNGEGFNTKVFWGHCINALVHSLILFWFPMKALEHDTVL
yeast_Drs2 1053 FTVWPPFVIGVFDQFVSSRLLERYPQLYKLGQKGQFFSVYIFWGWIINGFFHSAIVFIGTILIYRYGFAL
Consensus 413 ** * : -:::: : * ** : * : --- :-* - -
human_ATP11C 985 E-NGKVYGNWTFGTIVFTVLVFTVTLKLALDTRFWTWINHFVIWGSLAFYVFFSFFWGGIIWPFLKQQR-
human_ATP11A 994 S-NGQIFGNWTFGTLVFTVMVFTVTLKLALDTHYWTWINHFVIWGSLLFYVVFSLLWGGVIWPFLNYQR-
human_ATP8A1 970 G-NGKTSDYLLLGNFVYTFVVITVCLKAGLETSYWTWFSHIAIWGSIALWVVFFGIYSS-LWPAIPMAPD
human_ATP8A2 990 T-SGHATDYLFVGNIVYTYVVVTVCLKAGLETTAWTKFSHLAVWGSMLTWLVFFGIYST-IWPTIPIAPD
yeast_Drs2 1123 NMHGELADHWSWGVTVYTTSVIIVLGKAALVTNQWTKFTLIAIPGSLLFWLIFFPIYAS-IFPHANISRE
Consensus *- - * *:* *- * * -* * ** :- :-: **: ::-* ::- ::*
human_ATP11C 1053 MYFVFAQMLSSVSTWLAIILLIFISLFPEILLIVLKNVRRRSARRNLSCRRASDSLSARP----------
human_ATP11A 1062 MYYVFIQMLSSGPAWLAIVLLVTISLLPDVLKKVLCRQLWPTATERVQTK--SQCLSVEQ----------
human_ATP8A1 1038 MSGEAAMLFSSGVFWMGLLFIPVASLLLDVVYKVIKRTAFKTLVDEVQELEAKSQDPGAVVL----GKSL
human_ATP8A2 1058 MRGQATMVLSSAHFWLGLFLVPTACLIEDVAWRAAKHTCKKTLLEEVQELETKSRVLGKAVLRDSNGKRL
yeast_Drs2 1192 YYGVVKHTYGSGVFWLTLIVLPIFALVRDFLWKYYKRMYEPETYHVIQEMQKYNISDSRP----------
Consensus -* *: :--: -*- :- - :- -
human_ATP11C 1113 SVRPLLLRTFSDESNVL
human_ATP11A 1120 STIFMLSQTSSSLSF
human_ATP8A1 1104 TERAQLLKNVFKKNHVNLYRSESLQQNLLHGYAFSQDENGIVSQSEVIRAYDTTKQRPDEW
human_ATP8A2 1128 NERDRLIKRLGRKTPPTLFRGSSLQQGVPHGYAFSQEEHGAVSQEEVIRAYDTTKKKSRKK
yeast_Drs2 1251 -HVQQFQNAIRKVRQVQRMKKQ-------RGFAFSQAEEG--GQEKIVRMYDTTQKRGKYGELQDASANP
Consensus : -
yeast_Drs2 1312 FNDNNGLGSNDFESAEPFIENPFADGNQNSNRFSSSRDDISFDI

Fig. S4. Sequence alignment.

Primary sequences of indicated P4-ATPases isoforms were aligned using software MAFFT ver.7(35) and large gaps introduced in the non-conserved region were manually edited. Cytoplasmic domains (A, pink; P, green; N, light blue), secondary structures (α-helices, β-sheets and TM helices) and mutations introduced for the crystallized construct (ΔN7, ΔC38) are indicated above the alignment. The degree of conservation among evaluated sequences is indicated below the alignment. Acidic, basic, hydrophilic or hydrophobic amino acids are indicated as red, blue, green and black characters, respectively. Gene and protein ID are as follows; human ATP11C (NCBI:_XM_005262405.1), human ATP11A (Uniprot: P98196-1), human ATP8A1 (UniProt: Q9Y2Q0-2), bovine ATP8A2 (Genebank: GQ303567.3), and Saccharomyces cerevisiae Drs2 (UniProt: P39524-1).

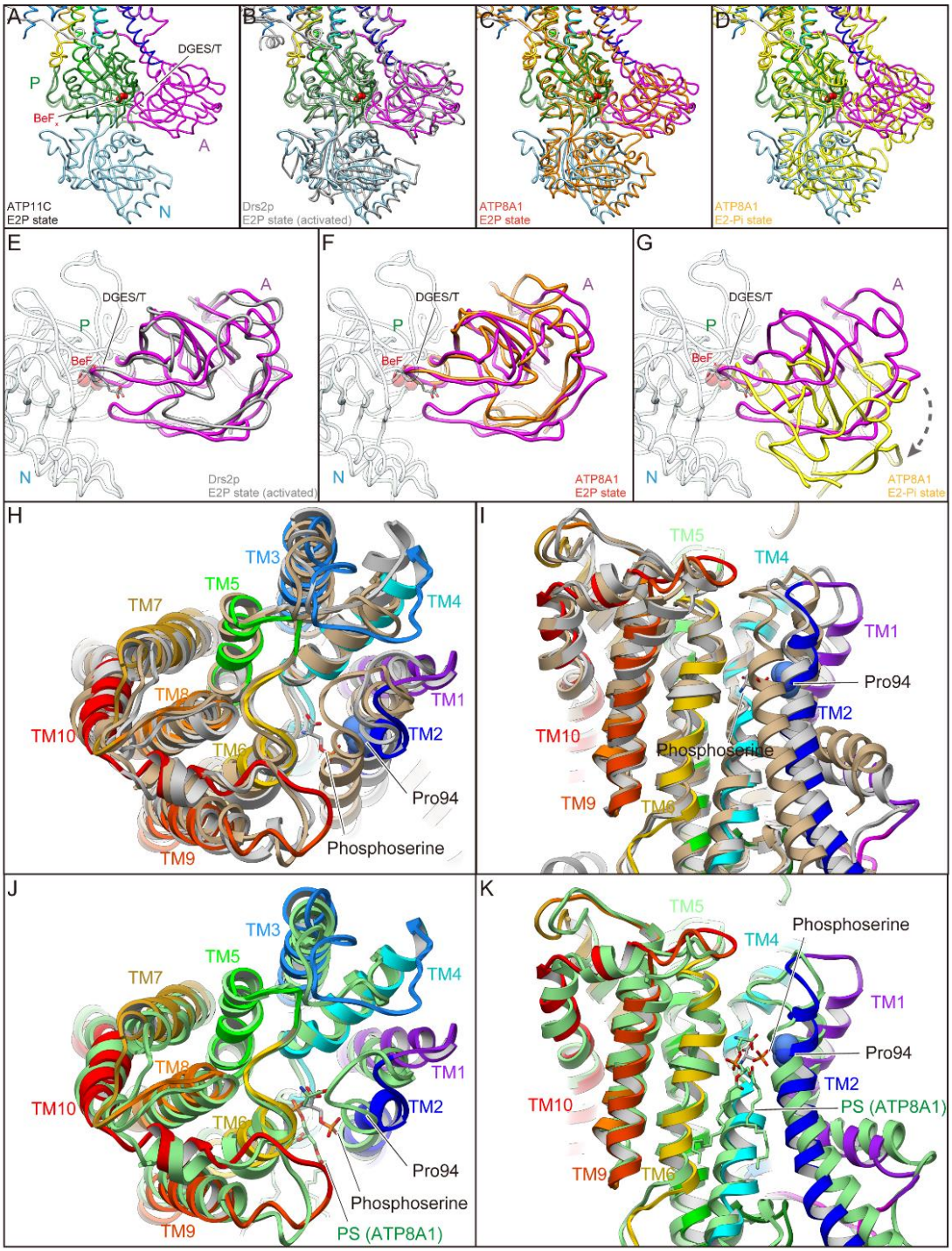

Fig. S5. Cytoplasmic domains

(**A-D**) Comparison of the relative orientations of the cytoplasmic domains viewed along with the membrane plane. Cytoplasmic domains of ATP11C are shown in worm models with the same color code as in Fig. 1C (**A**). Atomic models of Drs2p in E2P activated form (**B**, grey), ATP8A1 E2P form (**C**, orange) and ATP8A1 E2-P_i form (**D**, yellow) are superimposed on the ATP11C structure according to their P domain structures to show relative orientations of A and N domains. (**E-G**) Azimuthal position of the A domain is

compared. A domain of Drs2p (**E**), ATP8A1 E2P state (**F**) and E2-P_i state (**G**), and these models are superimposed on the ATP11C structure (only A domain is highlighted in magenta, and others are shown in transparent colors) as in A-D. Dotted arrow indicates the different azimuthal positions between ATP11C E2P state and ATP8A1 E2-P_i state. Phosphate analog BeF_x (red spheres) and DGES/T motif (sticks) in ATP11C structure are highlighted in all figures. (**H**-**K**) Comparison of the TM helix arrangement in ribbon representation. Atomic models of ATP11C E2P state (color codes as in Fig. 1), Drs2p E2P state (light grey) and ATP8A1 E2P state (tan) are aligned according to their TM helices (**H**,**I**). ATP8A1 E2-P_i transition state (light green) is also compared with ATP11C E2P state (**J**,**K**) Only catalytic subunits are shown in the figure, viewed from the exoplasmic side (**H**,**J**) or perpendicular to the membrane plane with exoplasmic side up (**I**,**K**). Phosphoserine (sticks) and Pro94 (spheres) in ATP11C, and PtdSer occluded in ATP8A1 E2-P_i state (sticks) are indicated in the figure.

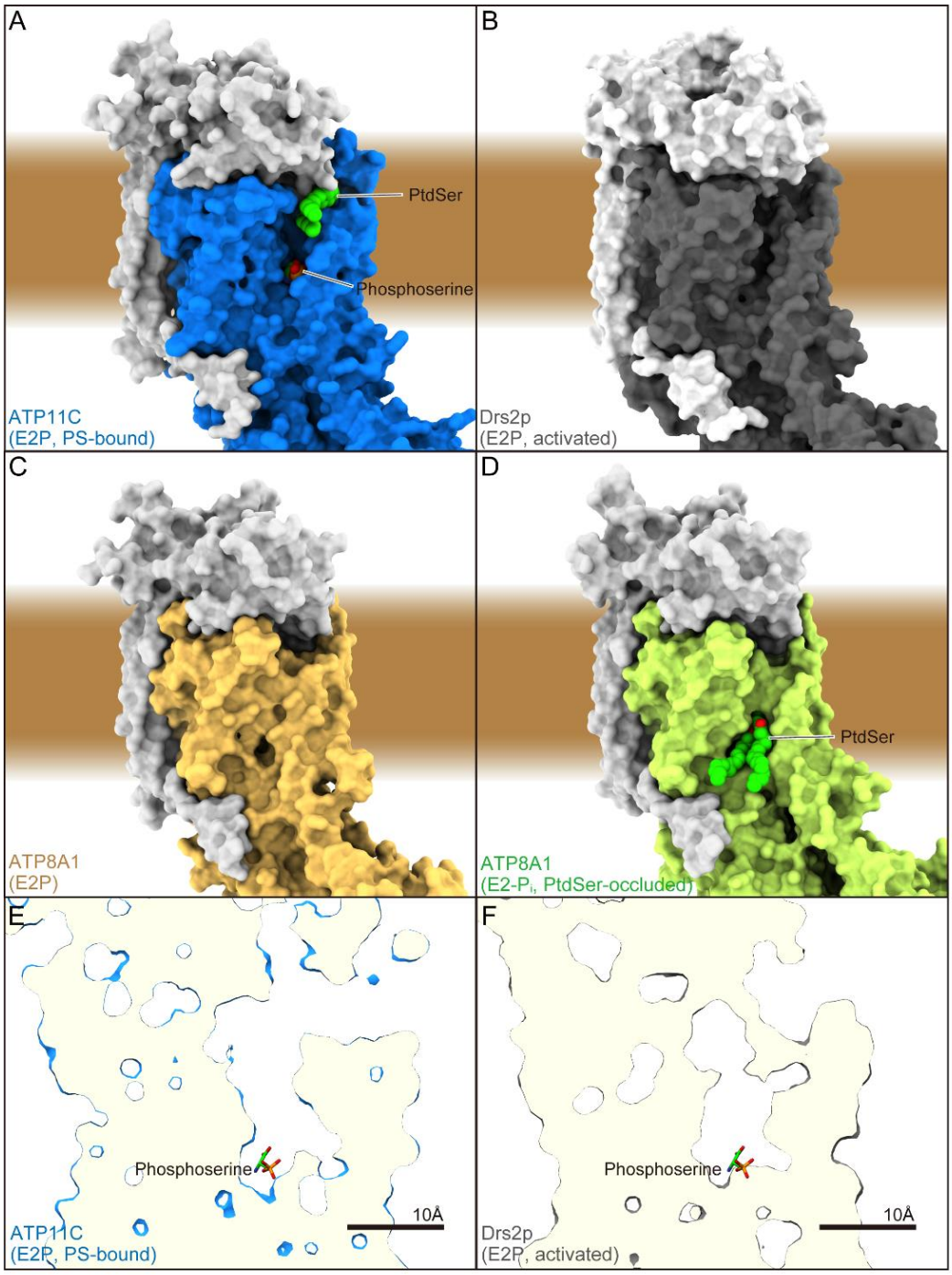

Fig. S6. Comparison of membrane crevices

(**A**-**D**) Surface representation of the atomic models of ATP11C E2P state (**A**), Drs2p E2P activated form (**B**), ATP8A1 E2P (**C**) and E2-P_i state (**D**). PtdSer and phosphoserine are indicated as spheres. Brown background indicates approximate location of the lipid bilayer. (**E**,**F**) Vertical sections of the TM region in ATP11C (**E**) and Drs2p (**F**) viewed from as in **A**-**D**. Phosphoserine (sticks) bound to the ATP11C and scale bar are shown for comparison.

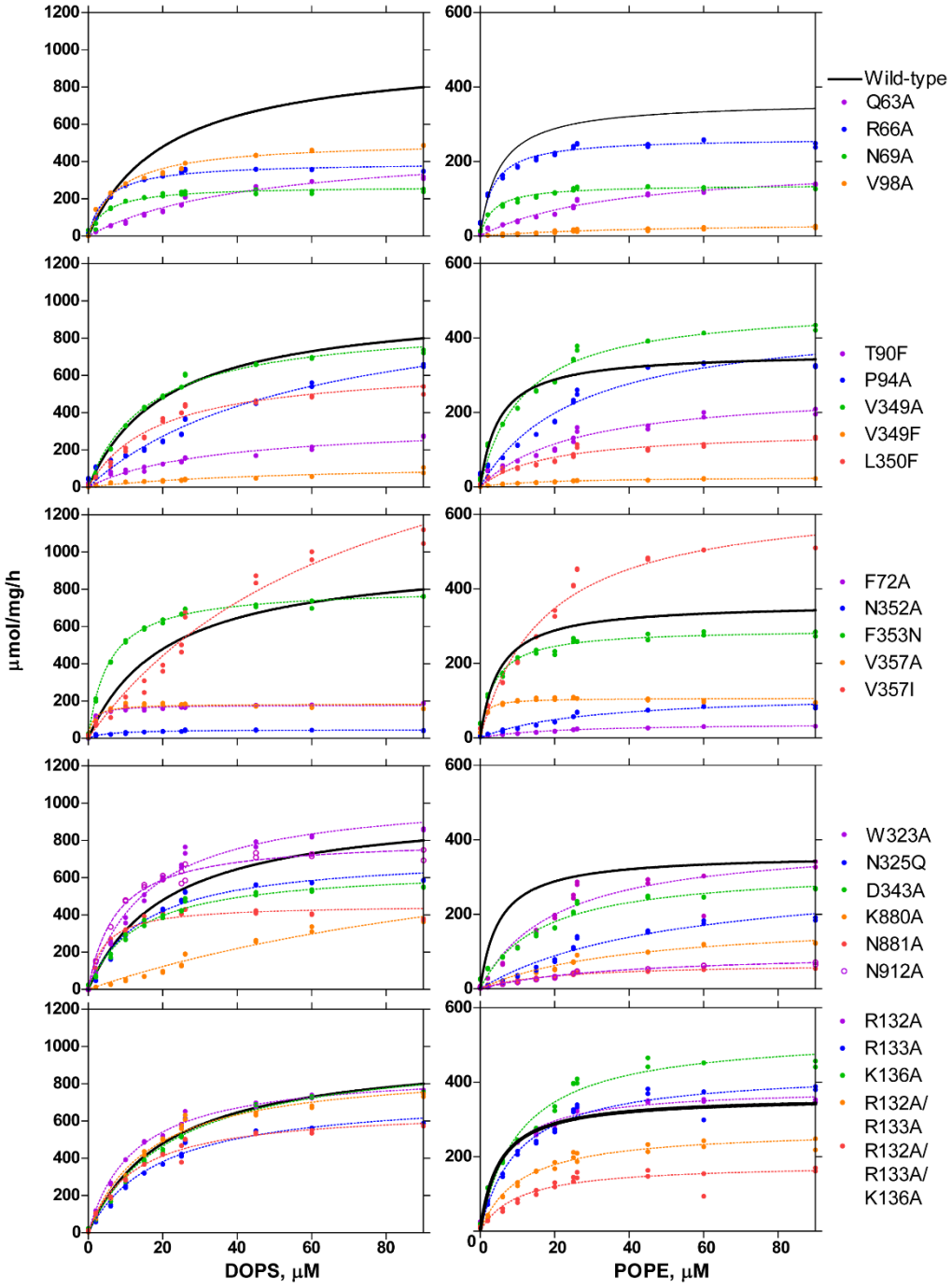

Fig. S7. Phospholipid-dependence of ATPase activity for mutants.
ATPase activities of indicated mutants are plotted as a function of DOPS (left) or POPE (right) concentration. Mutants are categorized as follows; cytoplasmic gate (1st row), surface of the membrane cleft (2nd row), occlusion site (3rd row), TM3-4 loop at exoplasmic cavity and residues in TM5 and 6 (4th row), and CDC50A exoplasmic domain facing the cavity (5th row). ATPase activity for the wild-type enzyme is shown in all graphs as a control (black lines).